


Formation of the Spectral Composition of the Output Voltage of Converters for Nuclear Magnetic Resonance

A. V. Zahranynnyi,  [0000-0003-2373-1896](https://orcid.org/0000-0003-2373-1896)

National technical university of Ukraine "Igor Sikorsky Kyiv Polytechnic Institute"  [00syn5v21](https://orcid.org/00syn5v21)
Kyiv, Ukraine

Abstract—In this paper, we consider the construction of an asynchronous control system for semiconductor converters for nuclear magnetic resonance. The relevance of research in this direction, main problems that arise during the construction of these systems are shown. Derived the mathematical model of the inverter, on the basis of which a control system with asynchronous pulse-width modulation is constructed. Proposed an equivalent converter circuit with a constant structure, constant parameters, and an equivalent EMF generator. Established correspondence between the equivalent circuit of the converter and its mathematical model in the form of differential equations. On the basis of mathematical equations, a structural diagram of the converter with a control system was developed and the principle of operation of the device was described according to it. To develop an algorithm for the control system, the dependence of the frequency change relative to the resonant frequency on the phase shift between the current through the filter and the voltage on the antenna circuit is determined. For which the model was built in Simulink and the corresponding simulation was carried out. Numerical dependences of reference signal frequency change and phase shift were obtained. The increase in efficiency of device for nuclear magnetic resonance is considered due to the use of multilevel inverters with tuning the frequency of operation to the frequency of the resonant circuit. Simulation of a three-level diode-clamped inverter showed that when the capacitance of the resonant circuit changes and, therefore, the resonant frequency of the circuit, the input current increases. The work obtained specific numerical dependencies. Time diagrams of voltages and currents on the main elements of the converter are given, which illustrate the implementation asynchronous pulse-width modulation in the control system. After working out the automatic frequency control algorithm, the increase in current consumption can be leveled off. The simulation results also show that it is possible to reduce the amplitude of the third harmonic. The disadvantages of the proposed system include the fact that the frequency of the converter is adjusted at each subsequent period of its operation. At the same time, the parameters of the filter can change again, which leads us to believe that adjusting the frequency will never give a 100% result, but will only allow to get as close as possible to the set parameters of the sounding signal. The work also indicates that it is possible to improve the spectral composition of the probing voltage generated by the converter by using more levels of a diode-clamped multi-level inverter. However, increasing the number of levels reduces the action speed of the system and complicates the control system itself. Therefore, the need to maintain a balance between the number of levels of the inverter and the complexity of the system is indicated.

Keywords: nuclear magnetic resonance; multilevel inverter; asynchronous pulse width modulation; mathematical model; control system; THD

I. INTRODUCTION

Maintaining the energy balance in the world is not only the most important, but also a very difficult task, because maintaining the currently achieved level of oil production, and even more so increasing it in the modern conditions of growing demand for energy resources, is also a non-trivial task. The success and effectiveness of the application of new oil production technologies in such conditions largely depends on the reliability and completeness of information about the physical properties of mineral deposits. One of the most effective and modern methods is nuclear magnetic resonance (NMR) [1]–[5]. NMR logging has earned a special place among other research methods due to its unique accuracy and complexity [6]–[9].

When developing systems for NMR, strict requirements are put forward for the accuracy of the envelope voltage (5%) and harmonic composition of the output probing voltage. One of the ways to meet these requirements is the use of multi-level inverters, which gives advantages in the power load of circuit components and greater possibilities of formation a various form of the output probing voltage. At the same time, a compromise is necessary between the complexity of the circuit (the number of inverter levels) and the harmonic composition of the output voltage.

The maximum power of the probing voltage, as well as the reduction of the content of higher harmonics, is achieved by the use of asynchronous pulse width modulation (asPWM) in the control system [10]–[19].



The purpose of the article is to develop a mathematical model of a multilevel inverter of the NMR-based logging system and its control system with automatic frequency adjustment to the frequency of the resonant circuit.

II. METHODS OF OBTAINING A MATHEMATICAL MODEL OF THE CONVERTER

Let's consider the formation of the equations of the mathematical model of the converter of the logging system using the example of a three-level inverter [20]–[25], the diagram of which is given in Fig. 1.

A stepped bipolar voltage with zero pauses is formed at the output of the inverter. When transistors VT_1 and VT'_2 are ON, a voltage $\frac{U}{2}$ is formed at the output, and when VT'_1 and VT_2 are ON — voltage $(\frac{U}{2})$. To form a zero pause on the load, it is necessary to turn on VT_1 and VT_2 .

During the operation of the device for nuclear magnetic resonance, the parameters of the oscillating circuit and the emitter change, which, in turn, causes a change the Larmor resonance frequency. Therefore, it is necessary to adjust the frequency of the converter to ensure a quasi-resonant mode to reduce dynamic losses.

In order to implement the asPWM, it is necessary to obtain mathematical equations that will describe the currents and voltages on the elements. Let's establish the correspondence between the equivalent circuit of the converter and its mathematical model in the form of differential equations. The equivalent circuit of the converter with a constant structure, constant parameters and a generator of the equivalent EMF $e(t)$, which can take the values $\frac{U}{2}$, $-\frac{U}{2}$ and 0, is shown in Fig. 2.

According to Kirchoff's first law, for the first node:

$$i_0(t) = i_{L_2}(t) + i_{C_2}(t) + i_R(t) \quad (1)$$

$$U_{C_2}(t) = U_{L_2}(t) = L_2 \cdot \frac{di_{L_2}(t)}{dt} = L_2 \cdot \frac{d[i_0(t) - i_{C_2}(t) - i_R(t)]}{dt} = L_2 \left[\frac{di_0(t)}{dt} - \frac{di_{C_2}(t)}{dt} - \frac{di_R(t)}{dt} \right] = L_2 \left[C_1 \cdot \frac{d^2 U_{C_1}(t)}{dt^2} - C_2 \cdot \frac{d^2 U_{C_2}(t)}{dt^2} - \frac{1}{R} \frac{dU_{C_2}(t)}{dt} \right] \quad (6)$$

Considering (6), let's write equations (2) and (3) in the form of a system:

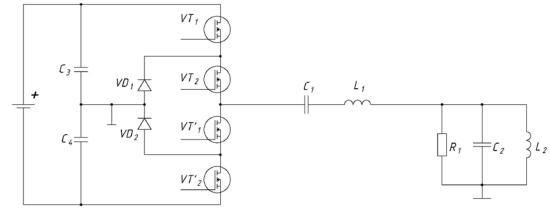


Fig. 1 The diode-clamped three-level inverter

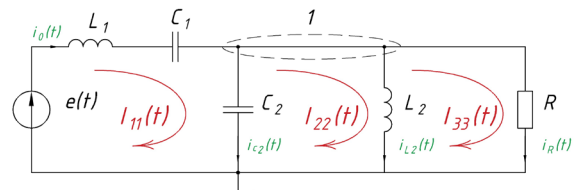


Fig. 2 The equivalent circuit of the converter with a constant structure, parameters and a generator of the equivalent EMF

Considering the current direction $i_0(t)$ and the direction of the first loop as indicated in Fig. 2, according to Kirchoff's second law, write:

$$L_1 \cdot \frac{di_0(t)}{dt} + U_{C_1}(t) + U_{C_2}(t) = e(t) \quad (2)$$

For the second and third circuits, taking into account the direction of the currents $i_{L_2}(t)$ and $i_{R_3}(t)$, as well as the directions of the branch currents, as indicated in the diagram, we write:

$$U_{C_2}(t) = U_{L_2}(t) \quad (3)$$

$$U_R(t) = U_{L_2}(t) \quad (4)$$

Let's express the current $i_{L_2}(t)$ from (1):

$$i_{L_2}(t) = i_0(t) - i_{C_2}(t) - i_R(t) \quad (5)$$

Taking into account that

$$i_0(t) = i_{L_1}(t) = i_{C_1}(t) = C_1 \cdot \frac{dU_{C_1}(t)}{dt} \quad \text{and}$$

$$U_{L_2}(t) = L_2 \cdot \frac{di_{L_2}(t)}{dt}, \text{ write:}$$

$$\begin{cases} L_1 \cdot C_1 \cdot \frac{d^2 U_{C_1}(t)}{dt^2} + U_{C_1}(t) + U_{C_2}(t) = e(t) \\ L_2 \cdot C_1 \cdot \frac{d^2 U_{C_1}(t)}{dt^2} - L_2 \cdot C_2 \cdot \frac{d^2 U_{C_2}(t)}{dt^2} - \frac{L_2}{R} \cdot \frac{dU_{C_2}(t)}{dt} - U_{C_2}(t) = 0 \end{cases} \quad (7)$$

Let's mark $L_1 \cdot C_1 = a_1$; $L_2 \cdot C_1 = a_2$; $L_2 \cdot C_2 = a_3$; $L_2 / R = a_4$.

It is obvious that for any structure of the passive part, the equivalent circuit of the converter with a constant structure, parameters, and generator of the equivalent EMF is described by a linear differential equation with constant coefficients and a piecewise continuous periodic function in the right-hand side.

Let's enter new variables:

$$\frac{dU_{C_1}(t)}{dt} = x(t), \quad \frac{dU_{C_2}(t)}{dt} = y(t). \quad (8)$$

Then:

$$\frac{d^2 U_{C_1}(t)}{dt^2} = \frac{dx(t)}{dt}, \quad \frac{d^2 U_{C_2}(t)}{dt^2} = \frac{dy(t)}{dt}. \quad (9)$$

Considering (8) and (9), we pass from the system of two differential equations of the second order (7) to the system of four differential equations of the first order with variables $x(t)$, $y(t)$, $U_{C_1}(t)$, $U_{C_2}(t)$:

$$\begin{cases} \frac{dU_{C_1}(t)}{dt} = x(t), \\ \frac{dU_{C_2}(t)}{dt} = y(t), \\ a_1 \cdot \frac{dx(t)}{dt} + U_{C_1}(t) + U_{C_2}(t) = e(t), \\ a_2 \cdot \frac{dx(t)}{dt} - a_3 \cdot \frac{dy(t)}{dt} - a_4 \cdot y(t) - U_{C_2}(t) = 0. \end{cases} \quad (10)$$

After mathematical transformations and simplifications, we write system (10) in matrix form:

$$\frac{dX(t)}{dt} = A \cdot X(t) + B \cdot e(t), \quad (11)$$

where

$$X(t) = \begin{bmatrix} U_{C_1} \\ U_{C_2} \\ x(t) \\ y(t) \end{bmatrix}, \quad A = \begin{bmatrix} 0 & 0 & 1 & 0 \\ 0 & 0 & 0 & 1 \\ -\frac{1}{a_1} & -\frac{1}{a_1} & 0 & \frac{1}{a_1} \\ -\frac{a_2}{a_1 \cdot a_3} & -\frac{a_1 + a_2}{a_1 \cdot a_3} & 0 & -\frac{a_4}{a_3} \end{bmatrix}, \quad B = \begin{bmatrix} 0 \\ 0 \\ \frac{1}{a_1} \\ \frac{a_2}{a_1 \cdot a_3} \end{bmatrix}.$$

Let's write down the final mathematical model in matrix form:

$$\begin{bmatrix} \frac{dU_{C_1}(t)}{dt} \\ \frac{dU_{C_2}(t)}{dt} \\ \frac{dx(t)}{dt} \\ \frac{dy(t)}{dt} \end{bmatrix} = \begin{bmatrix} 0 & 0 & 1 & 0 \\ 0 & 0 & 0 & 1 \\ -\frac{1}{a_1} & -\frac{1}{a_1} & 0 & \frac{1}{a_1} \\ -\frac{a_2}{a_1 \cdot a_3} & -\frac{a_1 + a_2}{a_1 \cdot a_3} & 0 & -\frac{a_4}{a_3} \end{bmatrix} \cdot \begin{bmatrix} U_{C_1} \\ U_{C_2} \\ x(t) \\ y(t) \end{bmatrix} + \begin{bmatrix} 0 \\ 0 \\ \frac{1}{a_1} \\ \frac{a_2}{a_1 \cdot a_3} \end{bmatrix} \cdot e(t) \quad (12)$$

III. RESULTS

To implement asynchronous pulse-width modulation when developing the structure of the control system, it

is necessary to supplement the mathematical model of the converter (12) with equations for the feedback voltage U_{fb} , the voltages of the output arms of the inverter U_{in1} and U_{in2} and their ratio.

$$\begin{cases}
 \frac{dU_{C1}(t)}{dt} = x(t), \\
 \frac{dU_{C2}(t)}{dt} = y(t); \\
 \frac{dx(t)}{dt} = \frac{1}{a_1} \cdot U_{C1}(t) + \frac{1}{a_1} \cdot U_{C2}(t) - \frac{1}{a_1} \cdot e(t); \\
 \frac{dy(t)}{dt} = -\frac{a_2}{a_1 \cdot a_3} \cdot U_{C1}(t) - \left(\frac{a_1 + a_2}{a_1 \cdot a_3} \right) \cdot U_{C2}(t) - \frac{a_4}{a_3} \cdot y(t) + \frac{a_2}{a_1 \cdot a_3} \cdot e(t); \\
 U_{33}(t) = \max\{|f(t)|\}_n, nT < t < (n+1)T; \\
 U_{in1} = \begin{cases} 1, nT + t_i \leq t \leq \frac{n+1}{2}(T + t_i); \\ -1, \frac{n+1}{2}(T + t_i) \leq t \leq (n+1)T + t_i; \end{cases} \\
 U_{in2} = \begin{cases} 1, nT \leq t \leq \frac{n+1}{2}T; \\ -1, \frac{n+1}{2}T \leq t \leq (n+1)T; \end{cases} \\
 e(t) = U_{in1} + U_{in2}.
 \end{cases} \tag{13}$$

where $\max\{|f(t)|\}_n$ – the maximum value of the module of the probing voltage $f(t)$ in the n -th period, t_i – moment of voltage change U_{fb} .

System (13) is the basis for the development of the control system of the converter with asPWM.

The structural diagram of the converter control system with asynchronous pulse width modulation is shown in Fig. 3.

The structural diagram includes: AB – accumulator battery; PS – power source; I – inverter, L – load, VS – voltage sensor, R – rectifier, AS – amplitude sensor, C – comparator, SVG – sawtooth voltage generator, PG – pulse generator, A – adder, PD – pulse distributor, BA – buffer amplifier.

The voltage from the battery AB is supplied to the inverter I. The multi-level inverter forms the sensing

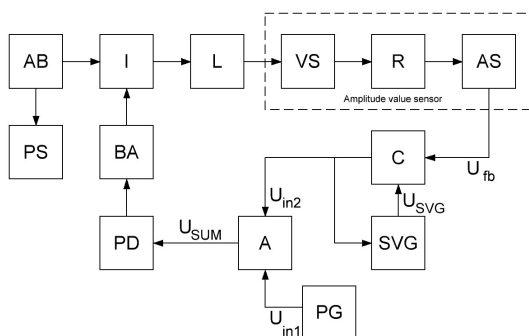


Fig. 3 The structural diagram of the converter control system with asynchronous pulse width modulation

voltage according to the control pulses. The stepped voltage from the inverter is converted into an amplitude-modulated sine wave using resonance filters. To ensure the quasi-resonance mode of operation of the device, it is necessary to generate a probing voltage with an accuracy of 5% [3]. For this, it is necessary to monitor the amplitude value of the modulated sinusoid on each half-cycle of the converter. The VS voltage sensor is a voltage divider, the voltage from which, after rectification, is fed to the AS amplitude sensor.

Fig. 4 shows the time diagrams of the three-level inverter circuit with asPWM.

The voltage U_{fb} from the amplitude sensor is compared with the USVG on comparator C. Since in asPWM systems the control angle is counted each time from

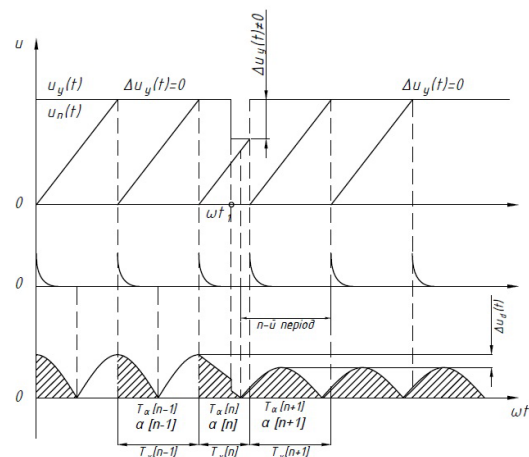


Fig. 4 The timing diagrams of the three-level inverter circuit with asPWM

the moment of the control pulse of the previous interval, the sawtooth voltage generator begins to unfold each subsequent period from the beginning of the previous control pulse. Thus, control pulses are formed at the output of the comparator, which are summed with the output pulses from the generator PG. The PD switching unit is designed to distribute control pulses across transistors. The BA amplifies the pulses to the required level to open the power transistors of the multi-level inverter.

In the event that, according to the SVG voltage, the duration of the pulse will exceed the duration of the period, its duration will be $T - \delta$, where T – duration of the standard period, δ – some minimum time interval to ensure a pause before the start of the next control pulse.

Timing diagrams illustrating the implementation of asPWM in the control system (see Fig. 3) are shown in Fig. 5.

The use of such a control system, which works according to the obtained mathematical ratios, allows you to ensure the necessary THD (Total Harmonic Distortion) indicators [26]–[30]. To check the performance of the system, a model of the converter with asPWM was developed in the MATLAB® Simulink® environment.

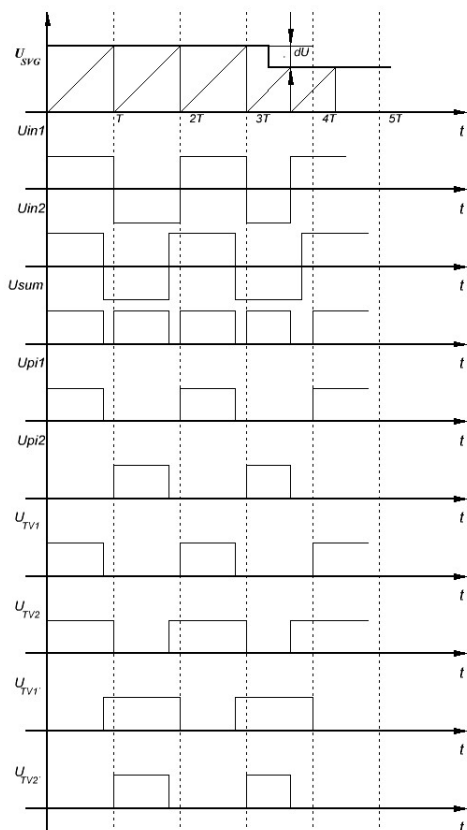


Fig. 5 The timing diagrams of the control system

The value of the phase shift at a change the frequency of the reference signal within $\pm 10\%$ was obtained (Table 1).

Simulations have shown that changing the capacitance of the resonant circuit by 4% (and therefore the resonant frequency of the circuit changes by 2%, from 500 kHz to 490 GHz) leads to an increase input current by 9.09% from 1.21 A to 1.32 A. Automatic frequency adjustment algorithm allow to level the increase in current consumption. The amplitude of the third harmonic also decreases from 17% (U_{m3}) to 6% (U'_{m3}) of the amplitude of the fundamental (Table 1).

TABLE 1 DEPENDENCE OF THE FREQUENCY CHANGE f_L ON THE PHASE SHIFT AND REDUCTION OF THE THIRD HARMONIC AFTER WORKING OUT AUTOMATIC FREQUENCY ADJUSTMENT ALGORITHM

f_L, Hz	$\Delta f, \text{Hz}$	$\varphi, ^\circ$	$U_{m3}, \%$	$U'_{m3}, \%$
490000	-10000	19,12	17,21	6,27
491000	-9000	17,50	16,36	6,25
492000	-8000	15,66	15,21	6,26
493000	-7000	13,69	13,87	6,24
494000	-6000	11,87	12,46	6,24
495000	-5000	9,75	11,34	6,23
496000	-4000	7,98	10,23	6,24
497000	-3000	5,90	9,11	6,23
498000	-2000	4,04	7,98	6,22
499000	-1000	2,01	7,12	6,22
500000	0	0,09	6,13	6,21
501000	1000	-2,01	7,11	6,21
502000	2000	-4,01	8,01	6,22
503000	3000	-5,90	9,02	6,23
504000	4000	-7,89	10,13	6,23
505000	5000	-9,71	11,41	6,24
506000	6000	-11,77	12,47	6,24
507000	7000	-13,52	13,94	6,25
508000	8000	-15,39	15,27	6,26
509000	9000	-17,11	16,38	6,26
510000	10000	-18,79	17,28	6,27

CONCLUSIONS

The obtained mathematical model of a multi-level inverter for nuclear magnetic resonance allows designing a control system of the converter based on asPWM.

The frequency adjustment allows to reduce current consumption by 9.09% and reduce third harmonic of the probe voltage from 17% to 6%. The obtained simulation results also show that it is possible to reduce the amplitude of the third harmonic when using a three-level inverter and an algorithm with automatic frequency adjustment by 11 percent.

REFERENCES

- [1] G. R. Coates, L. Xiao, and M. G. Prammer, *NMR Logging Principles and Applications*, 1st ed. Houston: Halliburton Energy Services, 2000.
- [2] T. Hassane, "Nuclear magnetic resonance and its applications for reservoir characterization," in *Applied Techniques to Integrated Oil and Gas Reservoir Characterization*, Elsevier, 2021, pp. 155–192. DOI: [10.1016/B978-0-12-817236-0.00005-4](https://doi.org/10.1016/B978-0-12-817236-0.00005-4)
- [3] P. J. Boul, R. Ramamoorty, P. N. Theologou, R. D. East, A. M. Drake, and T. Neville, "USE OF NUCLEAR MAGNETIC RESONANCE AND NEW CORE ANALYSIS TECHNOLOGY FOR DETERMINATION OF GAS SATURATION IN PRETTY HILL SANDSTONE RESERVOIRS, ONSHORE OTWAY BASIN," *The APPEA Journal*, vol. 39, no. 1, p. 437, 1999. DOI: [10.1071/AJ98025](https://doi.org/10.1071/AJ98025)
- [4] M. Tan, Y. Zou, and C. Zhou, "A new inversion method for (T₂, D) 2D NMR logging and fluid typing," *Comput Geosci*, vol. 51, pp. 366–380, Feb. 2013. DOI: [10.1016/j.cageo.2012.07.030](https://doi.org/10.1016/j.cageo.2012.07.030)
- [5] E. Toumelin and B. Sun, "Optimization of Wireline NMR Pulse Sequences," *Petrophysics*, vol. 52, no. 04, pp. 288–302, 2011. URL: <https://onepetro.org/petrophysics/article-abstract/52/04/288/171203/Optimization-of-Wireline-NMR-Pulse-Sequences?redirectedFrom=fulltext>
- [6] A. V. Zagranychnyi and V. V. Rohal, "Zastosuvannya inverteriv u prystroyakh yadernoho mahnitnoho rezonansu [Application the Inverters in Devices of Nuclear Magnetic Resonance]," *Tekhnichna Elektrodynamika*, no. 5, Aug. 2014. URL: <https://www.techned.org.ua/index.php/techned/article/view/1097/973>
- [7] A. V. Zahranychnii and V. V. Rogal, "Methods of forming voltage probing for devices nuclear magnetic resonance," *Electronics and Communications*, vol. 18, no. 5, pp. 19–24, Dec. 2013. DOI: [10.20535/2312-1807.2013.18.5.142741](https://doi.org/10.20535/2312-1807.2013.18.5.142741)
- [8] A. Tyshko and V. Popov, *Vysokochastotnyye preobrazovateli dlya ustroystv na osnove YAMR, rabotayushchikh pri povyshennykh temperaturakh [High-frequency converters for NMR-based devices operating at elevated temperatures]*, vol. 2. Kharkiv: Tekhnichna elektrodynamika. Silova Elektronika ta Energoeffektivnist, 2012.
- [9] R. Xie and L. Xiao, "Advanced fluid-typing methods for NMR logging," *Pet Sci*, vol. 8, no. 2, pp. 163–169, Jun. 2011. DOI: [10.1007/s12182-011-0130-4](https://doi.org/10.1007/s12182-011-0130-4)
- [10] V. E. Tonkal, V. S. Rudenko, V. Ya. Zhuikov, V. E. Suchik, S. P. Denisyuk, and A. V. Novoseltsev, *Ventil'nyye preobrazovateli s peremennoy strukturoy [Variable structure gate converters]*. Kyiv, Ukraine: Naukova dumka, 1990.
- [11] B. P. McGrath and D. G. Holmes, "Multicarrier PWM strategies for multilevel inverters," *IEEE Transactions on Industrial Electronics*, vol. 49, no. 4, pp. 858–867, Aug. 2002. DOI: [10.1109/TIE.2002.801073](https://doi.org/10.1109/TIE.2002.801073)
- [12] D. G. Holmes and T. A. Lipo, *Pulse Width Modulation for Power Converters: Principles and Practice*. Wiley-IEEE Press, 2003.
- [13] S. W. Shneen, F. N. Abdullah, and D. H. Shaker, "Simulation model of single phase PWM inverter by using MATLAB/Simulink," *International Journal of Power Electronics and Drive Systems (IJPEDS)*, vol. 12, no. 1, p. 212, Mar. 2021. DOI: [10.11591/ijpeds.v12.i1.pp212-216](https://doi.org/10.11591/ijpeds.v12.i1.pp212-216)
- [14] A. Tyshko, S. Balevicius, and S. Padmanaban, "An Increase of a Down-Hole Nuclear Magnetic Resonance Tool's Reliability and Accuracy by the Cancellation of a Multi-Module DC/AC Converter's Output's Higher Harmonics," *IEEE Access*, vol. 4, pp. 7912–7920, 2016. DOI: [10.1109/ACCESS.2016.2624498](https://doi.org/10.1109/ACCESS.2016.2624498)
- [15] K. Fathy et al., "PWM/PDM Dual Mode Controlled Soft Switching Multi Resonant High-Frequency Inverter," in *2005 IEEE International Conference on Industrial Technology*, pp. 1450–1455. DOI: [10.1109/ICIT.2005.1600863](https://doi.org/10.1109/ICIT.2005.1600863)
- [16] Xiaoyu Wang and W. Freitas, "Influence of Voltage Positive Feedback Anti-Islanding Scheme on Inverter-Based Distributed Generator Stability," *IEEE Transactions on Power Delivery*, vol. 24, no. 2, pp. 972–973, Apr. 2009. DOI: [10.1109/TPWRD.2009.2013373](https://doi.org/10.1109/TPWRD.2009.2013373)
- [17] H. Li, C. Liu, Y. Zou, and X. Jiang, "A Stability Improvement Method Based on Parameter Sensitivity for Grid-connected Inverter," in *IECON 2020 The 46th Annual Conference of the IEEE Industrial Electronics Society*, 2020, pp. 4649–4654. DOI: [10.1109/IECON43393.2020.9254964](https://doi.org/10.1109/IECON43393.2020.9254964)
- [18] "Invariant Probability Distribution of DC–DC Converters," in *Chaos Analysis and Chaotic EMI Suppression of DC-DC Converters*, Wiley, 2014, pp. 75–91. DOI: [10.1002/9781118451106.ch4](https://doi.org/10.1002/9781118451106.ch4)
- [19] X. Liu, A. M. Cramer, and F. Pan, "Generalized Average Method for Time-Invariant Modeling of Inverters," *IEEE Transactions on Circuits and Systems I: Regular Papers*, vol. 64, no. 3, pp. 740–751, Mar. 2017. DOI: [10.1109/TCSI.2016.2620442](https://doi.org/10.1109/TCSI.2016.2620442)
- [20] P. Rodriguez, M. D. Bellar, R. S. Muñoz-Aguilar, S. Busquets-Monge, and F. Blaabjerg, "Multilevel-Clamped Multilevel Converters (MLC₂)," *IEEE Trans Power Electron*, vol. 27, no. 3, pp. 1055–1060, Mar. 2012. DOI: [10.1109/TPEL.2011.2172224](https://doi.org/10.1109/TPEL.2011.2172224)
- [21] A. Yu. Manzhelii and A. V. Zagranychnyi, "Improving of the Probing Signal's Spectral Content for Devices Nuclear Magnetic Logging," *Microsystems, Electronics and Acoustics*, vol. 26, no. 2, pp. 237413-1-237413-5, Aug. 2021. DOI: [10.20535/2523-4455.mea.237413](https://doi.org/10.20535/2523-4455.mea.237413)
- [22] F. Z. Peng, J. W. McKeever, and D. J. Adams, "Cascade multilevel inverters for utility applications," in *Proceedings of the IECON'97 23rd International Conference on Industrial Electronics, Control, and Instrumentation (Cat. No.97CH36066)*, 1997, pp. 437–442. DOI: [10.1109/IECON.1997.671773](https://doi.org/10.1109/IECON.1997.671773)
- [23] D. G. Holmes and B. P. McGrath, "Opportunities for harmonic cancellation with carrier-based PWM for a two-level and multilevel cascaded inverters," *IEEE Trans Ind Appl*, vol. 37, no. 2, pp. 574–582, 2001. DOI: [10.1109/28.913724](https://doi.org/10.1109/28.913724)
- [24] F. Z. Peng and J.-S. Lai, "Multilevel cascade voltage source inverter with separate DC sources," US5642275A, 24-Jun-1997. URL: <https://patents.google.com/patent/US5642275A/en>
- [25] P. Lezana, J. Rodriguez, and D. A. Oyarzun, "Cascaded Multilevel Inverter With Regeneration Capability and Reduced Number of Switches," *IEEE Transactions on Industrial Electronics*, vol. 55, no. 3, pp. 1059–1066, Mar. 2008. DOI: [10.1109/TIE.2008.917095](https://doi.org/10.1109/TIE.2008.917095)
- [26] V. N. Nesterov and A. R. Li, "The Theory and Practice of Designing of Invariant Measurement Transducers and Systems Based on the Two-Channel Principle," *Izvestiya Samarskogo nauchnogo tsentra Rossiyskoy akademii nauk*, vol. 18, no. 4(7), pp. 1414–1422, 2016.
- [27] S. Patra, S. Agrawal, S. R. Mohanty, V. Agarwal, and M. Basu, "ESPRIT based robust anti-islanding algorithm for grid-tied inverter," in *2016 IEEE Students' Technology Symposium (TechSym)*, 2016, pp. 90–95. DOI: [10.1109/TechSym.2016.7872661](https://doi.org/10.1109/TechSym.2016.7872661)
- [28] J. R. Perez and P. C. Estay, *Predictive control of Power Converters and Electrical Drives*. Hoboken, NJ: Wiley-IEEE Press, 2012. ISBN: 978-1-119-96398-1
- [29] M. S. A. Dahidah, G. Konstantinou, and V. G. Agelidis, "A Review of Multilevel Selective Harmonic Elimination PWM: Formulations, Solving Algorithms, Implementation and Applications," *IEEE Trans Power Electron*, vol. 30, no. 8, pp. 4091–4106, Aug. 2015. DOI: [10.1109/TPEL.2014.2355226](https://doi.org/10.1109/TPEL.2014.2355226)
- [30] V. Y. Zhuykov, V. V. Rogal, and O. V. Budyonnyi, *Energetychna elektronika [Energetychna elektronika]*. Kyiv, Ukraine, 2009.



Надійшла до редакції 26 листопада 2023 року
Прийнята до друку 04 січня 2024 року


DOI: [10.20535/2523-4455.me.291566](https://doi.org/10.20535/2523-4455.me.291566)

УДК 621.316.72

Формування спектрального складу вихідної напруги перетворювачів ядерного магнітного резонансу

А. В. Заграничний,  [0000-0003-2373-1896](https://orcid.org/0000-0003-2373-1896)

Національний технічний університет України

«Київський політехнічний інститут імені Ігоря Сікорського»  [00syn5v21](https://doi.org/10.20535/2523-4455.me.291566)

Київ, Україна

Анотація—У даній роботі розглянуто побудову асинхронної системи керування напівпровідникових перетворювачів ядерного магнітного резонансу. Обґрунтовано актуальність досліджень, вказано основні проблеми та складнощі, які виникають при побудові таких систем. Виведено математичну модель інвертора, на основі якої побудовано систему керування з асинхронною широтно-імпульсною модуляцією. Запропоновано еквівалентну схему перетворювача з постійною структурою, постійними параметрами та еквівалентним генератором ЕРС. В роботі встановлено відповідність між еквівалентною схемою перетворювача та його математичною моделлю у вигляді диференціальних рівнянь. Для розробки алгоритму системи керування визначено залежність зміни частоти відносно резонансної частоти від зсуву фаз між струмом через фільтр і напругою на антенному контурі. Для чого була побудована модель у Simulink та проведено відповідне моделювання. Отримано чисельні залежності зміни частоти опорного сигналу та фазового зсуву. В статті розглянуто підвищення ефективності пристрою для ядерного магнітного резонансу за рахунок використання багаторівневих інверторів з налаштуванням частоти роботи. Моделювання трирівневого інвертора показало, що коли ємність резонансного контуру змінюється, а отже, і резонансна частота контуру, вхідний струм збільшується. Після відпрацювання алгоритму автоматичного підлаштування частоти збільшення споживаного струму можна нівелювати. Наведено часові діаграми напруг і струмів на основних елементах перетворювача, які ілюструють реалізацію асинхронної широтно-імпульсної модуляції в системі керування. Отримані результати моделювання також показують, що можна зменшити амплітуду третьої гармоніки. До недоліків запропонованої системи можна віднести те, що частота перетворювача регулюється на кожному наступному періоді його роботи. Робота також показує, що можна покращити спектральний склад зондувальної напруги, що генерується перетворювачем, використовуючи більше рівнів багаторівневого інвертора. Однак збільшення кількості рівнів знижує швидкість дії системи та ускладнює саму систему управління. Тому вказано на необхідність дотримання балансу між кількістю рівнів інвертора та складністю системи.

Ключові слова: *ядерно-магнітний резонанс; багаторівневий інвертор; асинхронна широтно-імпульсна модуляція; математична модель; система управління; THD*

